RLC-equivalent Circuit based Stub Loaded 2x2 MIMO Antenna for Wireless Applications

Atul Varshney, Vipul Sharma, Anuj Kumar Sharma

Abstract- **This communication offers a low-cost concave-shaped rectangular stub-loaded monopole 2x2 multi input multi output (MIMO) planar antenna for sub6GHz mid-band (N-78) and wideband wireless Wi-MAX applications. Two symmetrical reduced grounds are utilized to enhance the fractional bandwidth (FBW) and isolation factor. MIMO is further parasitically loaded with two rectangular stubs to tune the antenna close to the design frequency at 3.6GHz. The antenna possessed an Omni-directional radiation pattern (Peak gain of 3.38dBi and maximum radiation efficiency 92.82%) with a measured reflection coefficient (S_{11}) value lower than -10dB for a bandwidth 3.285-3.87GHz and excellent measured isolation coefficient (S_{12}) lower than -20dB using parasitic rectangular stubs and spatial distance approximately $\lambda_g/2$. All diversity parameters (CCL, DG, ECC, MEG, TARC, VSWR-MIMO, group delay) of this antenna are well below threshold values. The 2-port MIMO values of CCL<0.4bit/sec/Hz ensure a high data rate and DG close to 10dB confirms better reliability. The measured results show good closeness with simulated parametric graphs. The wideband impedance bandwidth is 14.87% (3.3-3.83GHz) for TARC lower than -10dB. That covers Sub-6GHz (N-78) mid-band (3.3-3.8GHz) and Wi-MAX (3.3-3.6GHz) applications. The RLC electrical equivalent circuit of the MIMO antenna is also discussed in this article.**

Keywords- **Channel Capacity Loss (CCL), Diversity Gain (DG), Envelope Correlation Coefficient (ECC), Isolation Coefficient (S_{12}), RLC equivalent circuit, Total Active Reflection Coefficient (TARC).**

I. INTRODUCTION

MIMO has been widely used in wireless RF communication for the past decade and a half to compensate for or overcome the diversity problem that exists in single-input single-output (SISO) systems. Furthermore, when compared to SISO antennas, the diversity features of MIMO ensure better reliability, high data rate, and high signal-to-noise ratio at the receiver end. G. Saxena et al. proposed a two-element tapered fed high diversity gain UWB-MIMO antenna with band notch characteristics in a compact size [1]. Doae El Hadri et al. proposed a MIMO antenna with two closely spaced radiating elements ($0.41\lambda_0$) with high isolation and low ECC for MIMO applications and 5G cellular mobile communications [2]. 5G technology operates in Sub-6 GHz (FR1<6GHz) and sub-24 GHz (FR2<24GHz) frequencies are normally falls under millimeter waves. There are many research activities in the literature relating to this topic for low frequencies (sub-6GHz) [3-6]. Milimmeter-waves are the most suitable candidate for 5G mobile communication to provide the requirement for superfast speeds up to 10 Gbps, [7]. Furthermore, higher channel capacity and data rates prerequisite wide bandwidth not only for mobile communication [8] perhaps also for other areas that influence our everyday life, such as transport, industry, media, and health. "5G is announced as the true enabler of Industry 4.0, which is considered to be the fourth industrial revolution technology" [9]. Md Nazmul Hasan, et al., have presented a bandwidth enhancement technique for rectangular monopole 2×2 and 4×4 MIMO antennas using DGS loaded with a U-shape stub that consists of two slits and a notch at optimized positions to enhance the impedance bandwidth and matching of the antenna [10]. Dinesh Yadav et al. have experimentally demonstrated, designed, and implemented high and uniform isolation single notched bands at 5.2GHz using complementary split ring resonator (CSRR) UWB two elements MIMO antenna. The high value of isolation has been achieved using a T-shaped stub [11]. Youngki Lee, et al. have proposed two elements of improved isolation MIMO antenna using an interdigital split ring resonator (SRR) on three FR4 substrates of 0.4mm thickness that consist of two inverted *L* strips and a ground plane [12]. Asim Quddus, et al. have presented a miniaturized UWB 2X2 MIMO antenna that comprises two decoupling structures, a strip line, and stepped rectangular radiators. The isolation enhancement is achieved by placing a slotted circular ring at the center of the ground plane placed between both antenna elements [13]. Jayshri Kulkarni and Chow-Yen-Desmond Sim have demonstrated a novel wideband cost-effective printed CPW-fed monopole oval-shaped 8X8 MIMO antenna for Wi-Fi5 and 6 applications [14]. Andrade-Gonzalez, E., A. et al. have presented high isolation along with stable TARC at random values of input signal phases, UWB applications, 2X2 MIMO antenna with parasitic elements using Fibonacci circles sequence, and DGS over the entire frequency range [15].

In this article, a low-cost simple compact edge fed rectangular parasitic loaded wideband 2X2 MIMO antenna using the reduced ground plane for sub-6GHz mid-frequency (N-78) band and Wi-MAX application with high diversity gain and isolation coefficient has been explained. The work comprises antenna design development methodology and detailed discussion on MIMO resultant diversity parameters, its fabrication, and testing and concluded with future remarks.

Article history: Received September 27, 2022; Accepted May 29, 2023.

Atul Varshney is with Electronics and Communication Department, FET, Gurukula Kangri (deemed to be) University, Haridwar, Uttarakhand, India, E-mail: atulgkvright@gmail.com, ORCID: 0000-0003-0440-4937

Vipul Sharma is with Electronics and Communication Department, FET, Gurukula Kangri University Haridwar, Uttarakhand, India, E-mail: vipul.s@rediffmail.com, ORCID: 0000-0002-5705-4259

Anuj Kumar Sharma is with Electronics and Communication Department, FET, Gurukula Kangri University Haridwar, Uttarakhand, India, E-mail: anujsharma@gkv.ac.in, ORCID: 0000-0003-0019-6421

II. MIMO Antenna Design Development and Methodology

The MIMO is fabricated on a piece of abundantly available low-cost FR-4 substrate of size 53.66mm x 24.0mm x 1.6mm with loss tangent 0.02 and permittivity of 4.4.

A. Design Equations

The proposed MIMO comprises two port edge-fed simple radiating patches, two rectangular stubs, and separate reduced ground structures. The 2x2 MIMO antenna is derived by replicating the single monopole single input single output (SISO) antenna element while maintaining the spatial distance between the two elements. The SISO antenna is designed at a frequency of 3.6GHz on an FR4 substrate with a relative loss tangent of 0.02, a thickness of 1.6mm, and dielectric permittivity $\varepsilon_r = 4.4$ using the basic design equations of conventional circular microstrip patch antenna [16-18]. Following are the design equations for the circular patch;

(i) Circular patch radius

$$a = \frac{F}{\{1+\frac{2h}{\pi\varepsilon_r F}[\ln(\frac{\pi F}{2h})+1.7726]\}^{1/2}} \quad (1)$$

where,

$$F = \frac{8.791\ X10^9}{f_r\sqrt{\varepsilon_r}} \quad (2)$$

(ii) Substrate and ground width and length

$$W_{gnd} = L_{gnd} = 2(\text{diameter}) = 2(2a) = 4a \quad (3)$$

(iii) Microstrip feed width

$$W_{feed} = \frac{7.48h}{e^{(Z_0\frac{\sqrt{\varepsilon_r+1}}{87})}} \quad (4)$$

The single-element SISO antenna is developed by using standard circular patch equ.1 and equ.2 and then converting this circular patch into a hexagonal ring-shaped polygon by selecting six numbers of segments. The initial patch radius of the SISO antenna is 14.1mm at an operating frequency of 3.6GHz. It is optimized for better tuning and reflection coefficients value with a good gain of 9mm. Finally, two circles of approximately the same reduced patch radius of the circular patch are arithmetically subtracted from the hexagonal polygon as mentioned in Fig 1. This is the main cause, why authors strongly considered the design Eq. (1) and Eq. (2) as the basic primarily root equations for the final geometry of the patch development.

B. Miniaturization Process and Development of Radiating Patch of SISO Antenna

The radius *a* for the main circular patch at the designed frequency calculated using Eq. (1) is 14.1mm, which results in the root size of the SISO with this radius being 56.4mm x 56.4mm (0.658 λ_0 x 0.658 λ_0). The optimization of patch radius is done for a better -10dB reflection coefficient with a high gain value of SISO over the full frequency band of interest. The final optimized radius of the patch at center C is 9.0mm. By selecting the number of segments 'Six' the circular patch is converted into a hexagonal patch. Miniaturization of radiating patch radius results in an excellent reduction in the overall area of the single-element patch. The radiating patch is developed by subtracting two circles centered at C_1 and C_2 of the same radius $a_1 = a_2 = 8.9$ mm (approximately equal to the patch radius $a = 9$mm). The patch is loaded with a parasitic rectangular stub to tune the antenna at the design frequency. The miniaturization process reduces the dimensions of SISO to 12mm x 24mm (0.14 λ_0 x 0.28 λ_0) and hence results in an 86.74% reduction in the SISO antenna area. This implies that 4.7-fold reduction along the width and a 2.35-fold reduction along the length of the final SISO. Step by step development process of the radiating patch is represented in Fig. 1.

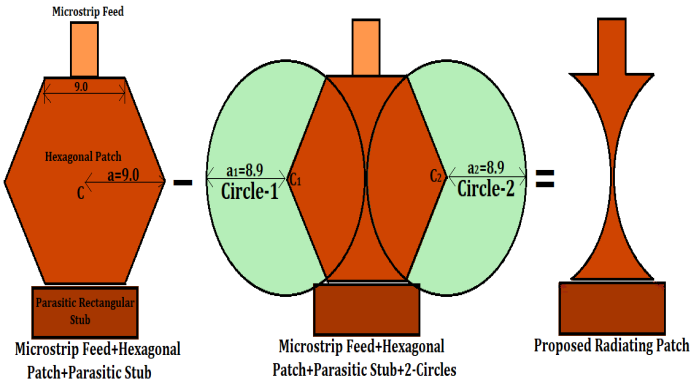

Fig. 1. Development of radiating patch for SISO antenna

C. Development of Radiating Patch of 2X2 MIMO Antenna

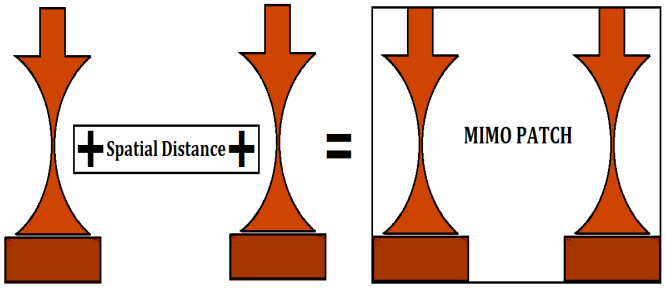

Fig. 2. Development of 2x2 MMO antenna radiating patch

The MIMO antenna radiating patch has been developed from the single element SISO antenna by just duplicating the structure at a suitable spatial distance *d* (not greater than guided half wavelength $\lambda_g/2$) so that a better decoupling of the one another (two elements) is maintained. This value is measured by the isolation coefficient S_{12} or S_{21} which must be lower than -10 dB for better performance of MIMO. Based on the above-mentioned criterion the radiating patch for the 2x2 MIMO antenna has been developed and illustrated in mathematical equation form in Fig. 2.

D. Effect of Rectangular Parasitic Stub Load on 2-Port MIMO Antenna

The two-port antennas without parasitic load are first developed and for fine-tuning purposes, the two ports MIMO antenna is further loaded with parasitic rectangular stubs. Their reflection coefficients (S_{11}) and isolation coefficients (S_{12}) comparison are represented in Fig. 3. It is concluded from the comparison curves that the value of reflection and isolation coefficients are well below the -20dB line. Without a rectangular parasitic load the antenna resonates at 3.75GHz and by the addition of parasitic stub load in MIMO the resonating frequency shifts towards the left and tunes the antenna to operate at 3.5GHz which is near the design frequency of 3.6GHz. The effect of the insertion of the parasitic load is depicted by dashed lines in Fig. 3.

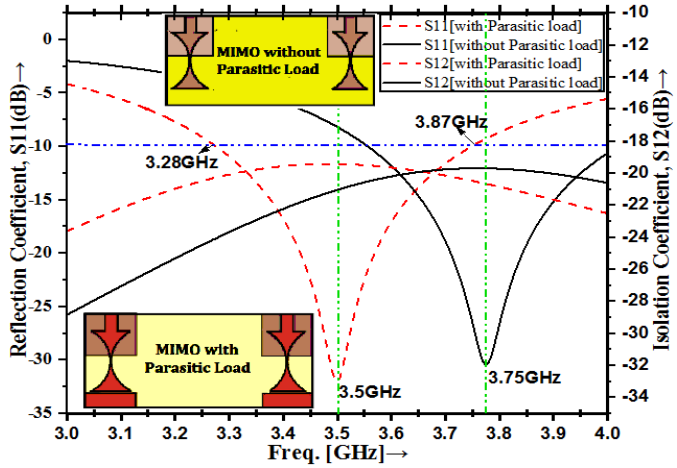

Fig. 3. Effect of parasitic rectangular stub load

E. Optimized Design Parameters of 2x2 MIMO Antenna

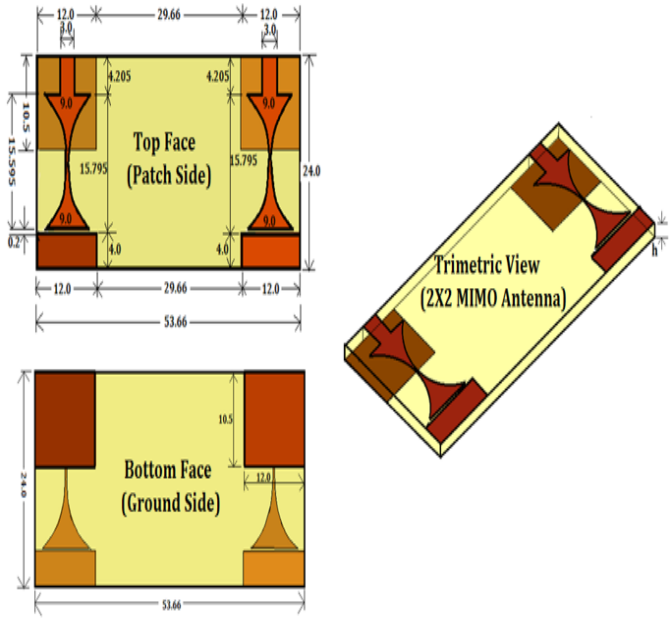

Fig. 4. Concave-Shaped 2x2 MIMO antenna (top view, bottom view, and trimetric view), all the dimensions are in mm

All design parameters of the two port MIMO antenna are optimized for larger antenna gain and impedance bandwidth, as well as better reflection coefficient S_{11} and isolation coefficient S_{12}, which both should be lower than -10dB at the design frequency and the specified frequency range of span. Final optimized dimensions of the top, bottom, and trimetric view (measured in mm) of the MIMO geometries have been depicted in Fig. 4, respectively and the description and designation of the corresponding parameters with optimized values are mentioned in Table I.

TABLE I
OPTIMIZED DIMENSIONS OF 2X2 MIMO ANTENNA

Parameter Name	Designation and Description	Values (mm)
L_{sub}	Substrate Length	53.66
W_{sub}	Substrate Width	24.0
L_{gnd}	Reduced ground structure Length	10.5
W_{gnd}	Reduced ground structure Width	12.0
L_{stub}	Parasitic Rectangular Stub Length	4.0
W_{stub}	Parasitic Rectangular Stub width	12.0
L_{feed}	50Ω Microstrip Feed Length	4.205
W_{feed}	50Ω Microstrip Feed Width	3.0
W_{patch}	Width of Patch	9.0
L_{patch}	Length of Patch	15.595
L_{arc}	Length of Patch Arcs	18.64
a	Radius of Patch Arcs	8.9
G	Gap between Patch and Parasitic Rectangular Stub	0.2
D	Distance between two Patches “Spatial Distance”	29.66
h	Substrate Thickness	1.6

F. Prototype of 2x2 MIMO Antenna

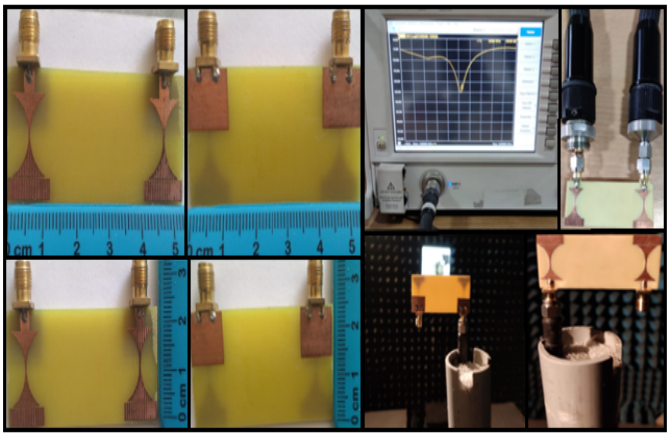

Fig. 5. Prototype of the concave-shaped 2x2 MIMO antenna (Left half) and their parameters testing and measurements (Right half)

Finally, the optimized 2-port edge fed 2x2 MIMO antenna with size 53.66mm x 24mm x 1.6mm is fabricated on low-cost, low-profile FR-4 Substrate by photolithography and etching process. The final photographs of the prototype MIMO antenna are shown in the left section of Fig. 5 and their reflection coefficient measurements using a vector network analyzer (Agilent Technologies N5247A), gain,

radiation pattern (in an anechoic chamber), and other parameter measurements also shown in the right half of Fig. 5.

III. Results and Discussions

A. Reflection Coefficient (S_{11}) and Isolation Coefficient (S_{12})

The scattering parameters of measured versus simulated results are depicted in Fig. 6. The measured reflection coefficient (S_{11}) of the proposed MIMO antenna is below -10dB for the whole N-78 band of sub-6GHz from 3.30 to 3.80 GHz as shown in Fig. 6 (Left-hand vertical scale). The measured isolation coefficient (S_{12}) is superior to the simulated value of S_{12} (Right-hand vertical scale). Both measured and simulated Isolation coefficient values are well below the threshold value -15dB. The measured isolation between the two element antenna radiating patches is lower than -30dB over the entire wideband of interest 3.0 to 4.0 GHz. This high value of the isolation coefficient ensures the guarantee of better decoupling and reliability of signal reception by the two antenna elements of the 2x2 MIMO system.

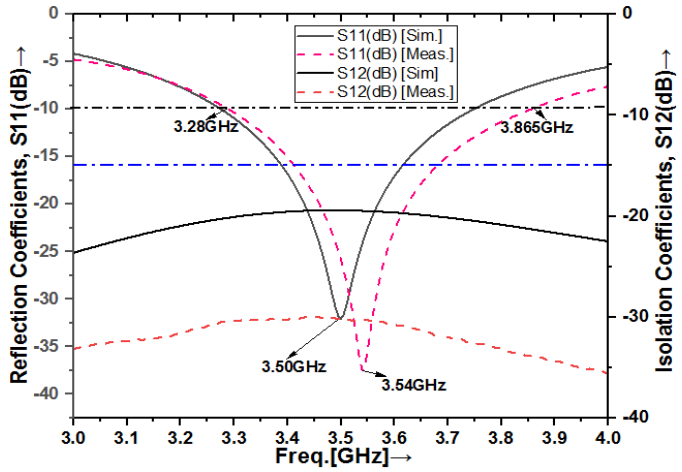

Fig.6. Simulated and measured reflection coefficients (S_{11}) and isolation coefficients (S_{12})

B. Diversity Performance Parameters

Any MIMO antenna is characterized by its diversity performance parameters. There are mainly six major diversity parameters that are derived from primary S-parameters, "total active reflection coefficient (TARC), VSWR-MIMO, envelope correlation coefficient (ECC), diversity gain (DG), mean effective gain (MEG), channel capacity loss (CCL)". Some other additional MIMO antenna parameters exist like, "radiation efficiency, multiplexing efficiency, group delay, a roll of criteria (RoC), and cross-correlation coefficient" etc.

B.1. TARC and VSWR-MIMO

The measured TARC and VSWR-MIMO values are derived from the measured S-parameter value using a standard multi-port MIMO antenna equation [1, 11] and plotted along with simulated TARC and VSWR-MIMO of concave-shaped 2x2 MIMO antenna as represented in Fig. 7 (left vertical scale) and Fig. 7 (right vertical scale), respectively. These diversity performance parameters are responsible parameters for determining the impedance bandwidth and hence suitable applications. The TARC magnitude less than zero (TARC<0) means the MIMO antenna is suitable for diversity applications. The measured TARC lower than -10dB for an impedance bandwidth 3.30-3.89GHz and the corresponding value of VSWR-MIMO less than 2 exists for an impedance bandwidth from 3.30-4.0GHz. This ensures the proposed MIMO antenna is suitable for N-78 band operations, sub-6GHz, and Wi-MAX applications.

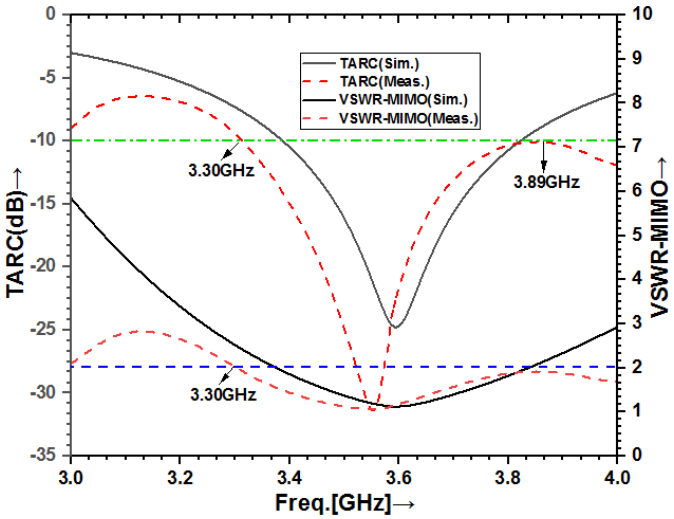

Fig.7. TARC curves and VSWR-MIMO plots of 2x2 MIMO

B.2. ECC, CCC, and DG

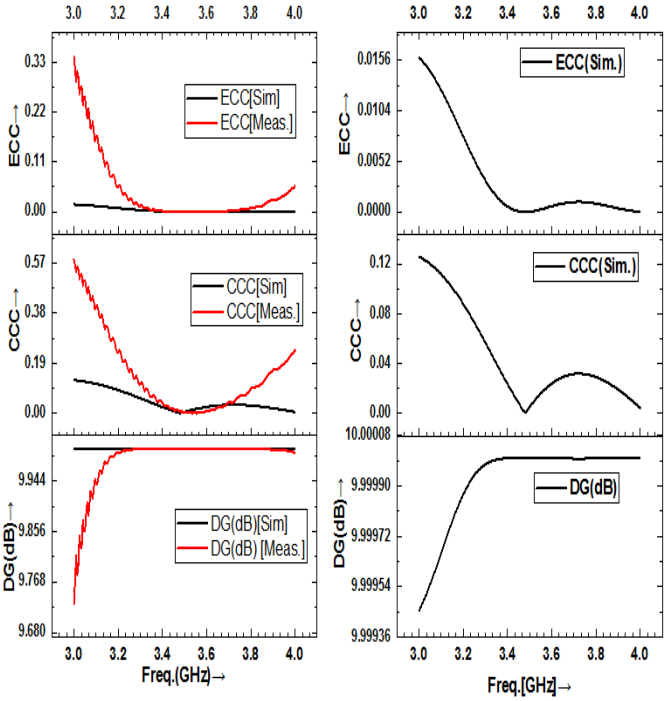

Fig. 8. Correlation coefficients ECC, CCC curves, and diversity gain (DG) plots (Left side) and their zoomed simulated plots (Right side)

Transmission, diversity gain, correlation, and TARC are used for the evaluation of the MIMO antennas. The ECC is derived from measured scattering parameters using standard equations [1, 11 and 19] and plotted along with simulated ECC as shown in Fig 8 (left top). It is observed from the graph that the simulated ECC is lower than 0.016 whereas most of its measured value is lower than 0.3. An ECC value less than 0.3 is considered pretty good and less than 0.1 should be selected for better isolation. The CCC is just derived by taking the square root of ECC ($CCC = \sqrt{ECC}$) and also plotted concerning a frequency just below the ECC plot in Fig 8 (left side) [20]. The DG is also derived from ECC [18] and it is better if it is close to 10dB as shown in Fig. 8 lowest plot. The DG value >9.95dB ensures reliability and guarantees the signal reaches the receiver or has better transmission reliability. The enlarged curves of ECC, CCC, and DG are shown to the right in Fig 8.The simulated ECC, CCC, and DG curves are looking flat concerning measured similar diversity parameters. One of the major reasons is the low-frequency range of interest i.e. 1GHz, very good reflection coefficients, and isolation coefficient i.e. good decoupling between the two antenna elements of 2x2 concave shape MIMO. Another big cause of the flatness of curves is the shape of the antenna elements i.e. concave shaped. The deepest point-to-point horizontal distance between two concave-shaped antenna elements is more than the spatial distance between two antenna elements.

B.3. Channel Capacity Loss (CCL)

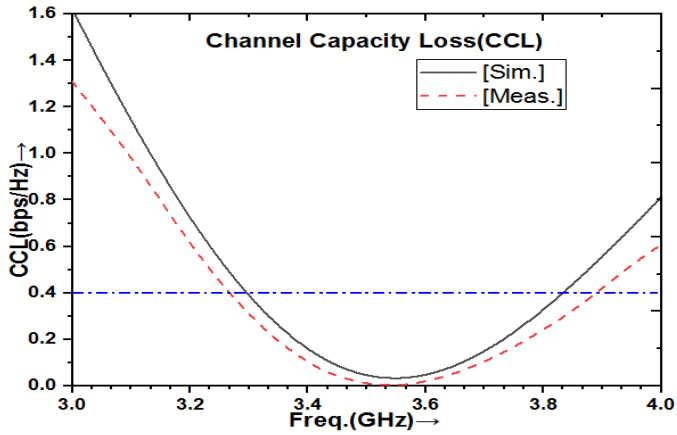

Fig. 9. CCL curve of concave-shaped MIMO

It is desirable for MIMO operation that the CCL value should be < 0.4 bps/Hz [21]. The one more diversity parameter CCL is ~~also~~ evaluated using measured S-parameters by taking the negative log (at base two) of the magnitude of determinants of the correlation matrix [1, 11, and 22] and plotted with simulated CCL as shown in Fig 9. It is found in good agreement with simulated one and CCL is well below under 0.4bit/sec/Hz for the whole N-78 band (3.3-3.8GHz). The proposed antenna offers better diversity results and a high data rate (BER) in terms of CCL.

B.4. Mean Effective Gain (MEG)

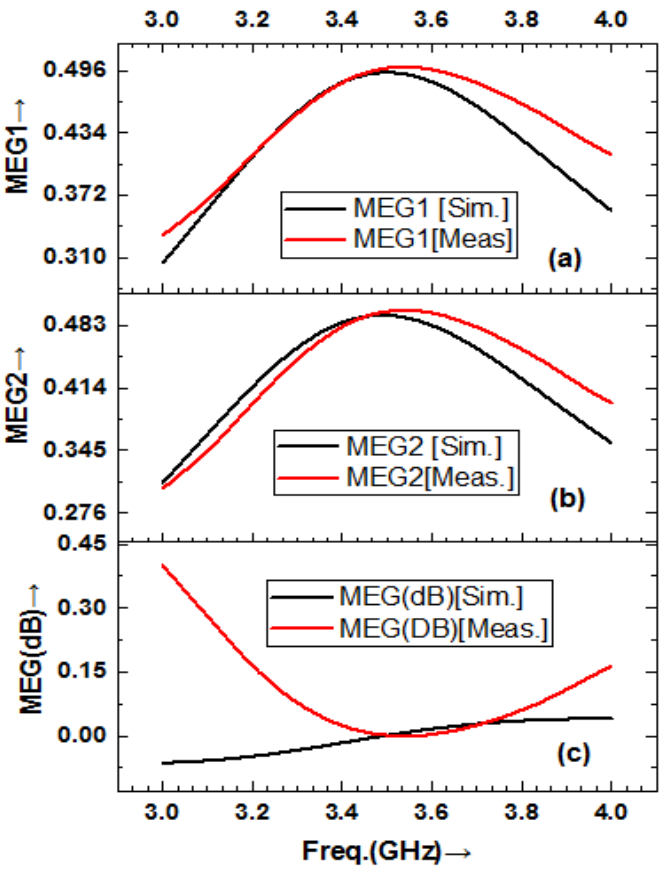

Fig. 10. (a) MEG curve at port1, (b) MEG curve at port 2, and (c) MEG curve

The MEG is defined for each port as "the ratio of the mean received power by the i^{th} antenna to the mean incident power of the j^{th} antenna with the same route" [1, 11, and 29]. The overall MEG of the two by two MIMO antennas is the ratio of the MEG1 and MEG2 while it is a difference of MEG1 and MEG2 in dB values. Mathematically, the MEG, MEG1, and MEG2 are defined as

$$\mathrm{MEG} = \frac{\mathrm{MEG_1}}{\mathrm{MEG_2}}$$

or

$$\mathrm{MEG\ (dB)} = MEG_1(\mathrm{dB}) - \mathrm{MEG_2(dB)} \tag{5}$$

In general, for any port MIMO antenna, the MEG is defined as [29]

$$\mathrm{MEG_i} = 0.5\left[1 - \sum_{j=1}^{N}|S_{ij}|^2\right] \tag{6}$$

For, 2x2 MIMO antenna MEG1 and MEG2 is defined as [29]

$$\mathrm{MEG_1} = 0.5[1 - |S_{11}|^2 - |S_{12}|^2] \tag{7}$$

$$\mathrm{MEG_2} = 0.5[1 - |S_{21}|^2 - |S_{22}|^2] \tag{8}$$

$$\mathrm{MEG_i} = |\mathrm{MEG_i} - \mathrm{MEG_2}| < 3\mathrm{dB} \tag{9}$$

Both measured and simulated values of MEG at ports 1 and 2 are in good concurrence with each other as represented in Fig 10 (a-c). Measured MEG values are in good agreement with simulated values and well below 0.5 dB. "The imbalance levels of the diverse broadcast divisions are measured in terms of MEG" [21]. The MEG is considered a better choice if it lies between -3dB and +3dB. The MEG_1 and MEG_2 are identical and their ratio is close to unity which satisfies the criterion of 'identicalness' of two antennas [22].

B.5. Radiation Efficiencies at Port 1 and Port 2

The radiation efficiency at Ports 1 and Port 2 is determined from the measured mean effective gain (MEG) values by using the relation [23],

$$MEG_i = 0.5\eta_{i,rad}. \quad (10)$$

where, $\eta_{i,rad}$. is the radiation efficency at i^{th} port.

Therefore, the radiation efficiencies at Port 1 and Port 2 are defined in terms of MEG1 and MEG2, and are evaluated from MIMO antenna S-parameters values by the following relations [23],

$$\eta_{1,rad} = 1 - |S_{11}|^2 - |S_{12}|^2 \quad (11)$$

$$\eta_{2,rad} = 1 - |S_{21}|^2 - |S_{22}|^2 \quad (12)$$

$$\eta_{rad} = \eta_{1,rad} \times \eta_{2,rad} \quad (13)$$

where $\eta_{1,rad}$ and $\eta_{2,rad}$ are the radiation efficiencies at Port1 and Port2 respectively and η_{rad} is the total radiation efficiency. The radiation efficiencies are plotted with simulated radiation efficiency for Port 1 and Port 2 in Fig 11(a) and Fig 11(b), respectively. Both the radiation efficiencies are found in concord. The measured value of radiation efficiency lies between 0.67 and 0.9995 for both ports. Ideally, efficiencies close to 1 are preferable but MIMO antennas designed with frequencies more than 60% are good-designed MIMO [23].

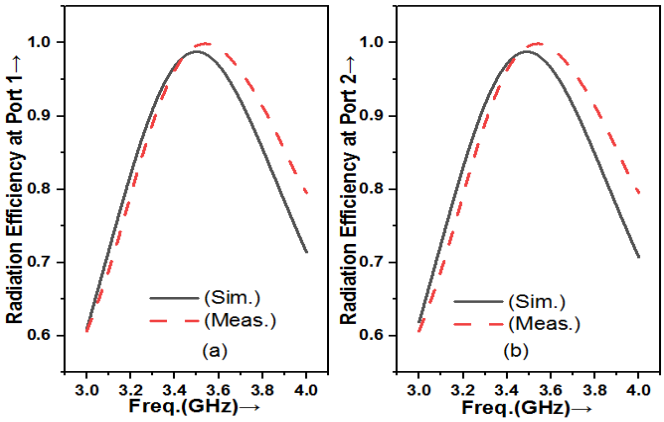

Fig.11. (a) 2X2 MIMO Radiation efficiency at port 1 and (b) radiation efficiency at port 2

B.6. Group Delay, τ_g (ns)

Group delay is defined as negative of the rate of change of phase angle concerning angular frequency. Mathematically the Group delay is given by

$$T_d = -\frac{d\Phi}{d\omega} \quad (14)$$

where Φ is the phase angle of S_{12} or S_{21} corresponding to transmission coefficients (S_{12t} or S_{21t}) and ω is the frequency in rad/s [1]. Finally, the time domain analysis of the proposed MIMO antenna is verified by locating two similar antennas in front of each other (one as a receiver and the other as a transmitter) at 100cm apart and then group delay (ns) is analyzed. The simulated group delay deviation of the proposed concave-shaped MIMO antenna is ≤ 0.72 ns over the entire wideband (Sub-6GHz N-78 band). The simulated group delay is displayed in Fig. 12. It is noticed from the group delay plot that for transmission coefficient S_{12t} or S_{21t} is found positive. This group delay for transmission coefficient S_{12t} or S_{21t} is generally considered the main group delay for the 2X2 MIMO system [24]. A lower value of the isolation coefficient may also be one of the important causes of negative group delay [25]. This will generally affect the group delay caused by S_{12t} or S_{21t}.

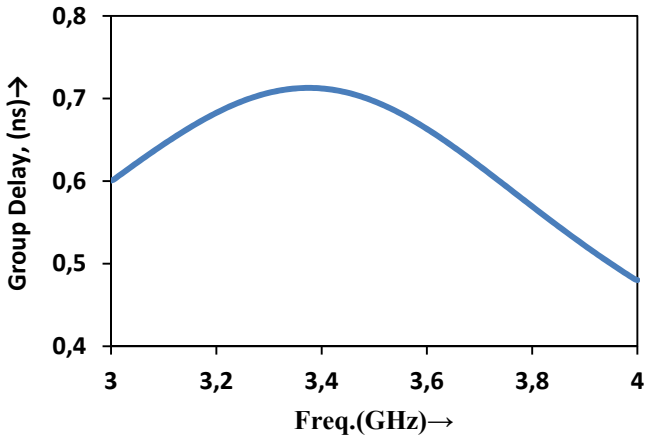

Fig.12. Group delay of MIMO

C. Radiation Patterns

The concave-shaped antenna has an Omnidirectional radiation pattern as illustrated in Fig. 13(a) and Fig. 13(b). Fig. 13(a) depicted the 3D-radiation pattern of the single-element SISO antenna whereas the gain of the proposed 2X2 MIMO is depicted in Fig. 13(b). In these figures, the total realized gain (dB) is represented in theta and phi planes. The horizontal plane represents the phi 0° plane while the vertical plane represents the theta 0° plane. It has been noticed from the radiation pattern that the antenna radiated above the patch and below the ground plane and hence possesses the Omnidirectional radiation pattern. The maximum gain of SISO and 2x2 MIMO antennas are evaluated using the following relationships [16],

$$G\,(dBi) = 2.15 + G\,(dB) \quad (15)$$

where, $$G\,(dB) = 10\log(\eta_{rad} \times \frac{41257^{\blacksquare}}{\theta_E^{\circ} \times \theta_H^{\circ}}) \quad (16)$$

where θ_E° and θ_H° are the half power beam width (HPBW) in E-plane and H-plane radiation patterns and η_{rad} is the total radiation efficiency as in Eq. (13). The HPBW for the SISO antenna are 360° and 88° respectively evaluated from Fig.s 13 (b), and the total radiation efficiency of the SISO antenna was evaluated as 0.956. The HPBW for the MIMO antenna are 360° and 80° respectively evaluated from Figs 13 (d), (i) and (ii), and the total radiation efficiency of the MIMO antenna was evaluated as 0.9282. Therefore, the maximum gain obtained with the SISO antenna is 3.05dBi whereas that of with MIMO antenna is 3.38dBi at frequency3.6GHz. Thus we can say that the use of MIMO not only improves the single-element antenna data rate diversity parameters but it also improves the gain of the SISO antenna. The polar plot of realized gain in E-Plane (XY-plane), and H-Plane (YZ-plane) with φ=0˚, φ=90˚ at 3.6GHz are shown in Fig. 13(c). In H-plane the pattern of gain is like a figure of eight ("8") whereas the polar radiation plot in E-plane is equally radiator. The simulated E-plane and H-plane patterns are compared with measured (E-plane and H-plane) radiation plots and found in a good quality match in shape and maximum magnitude.

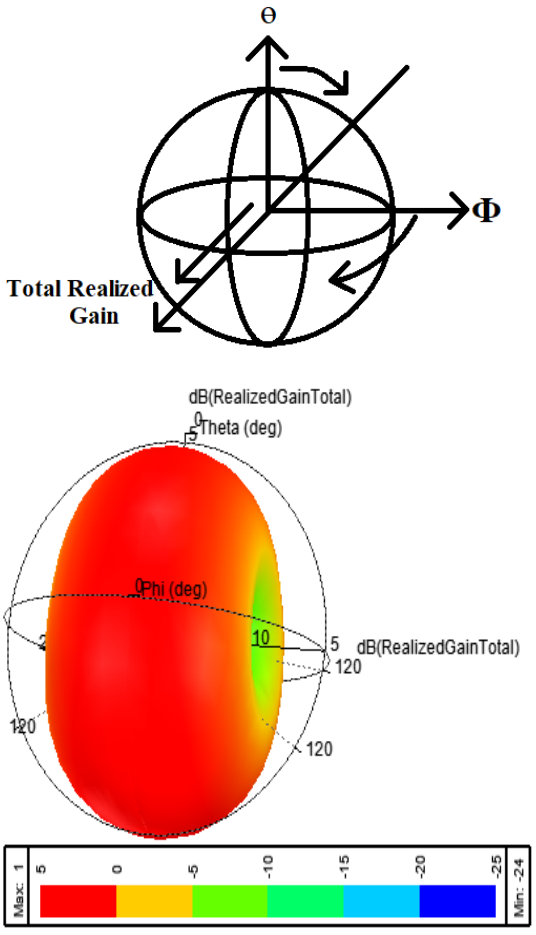

(a)

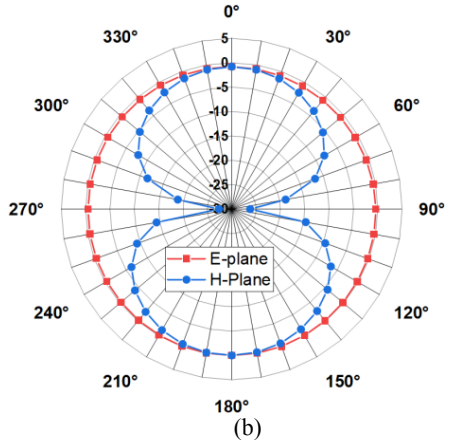

(b)

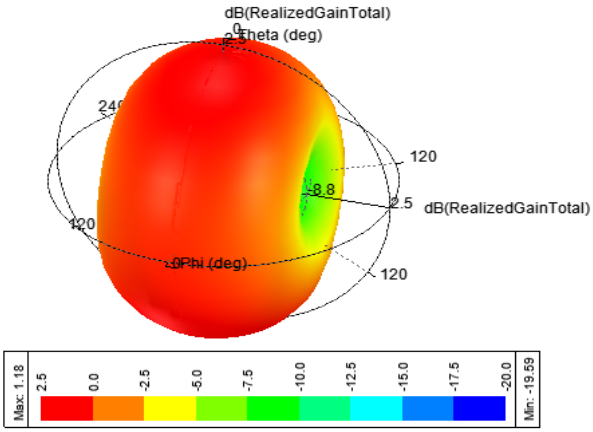

(c)

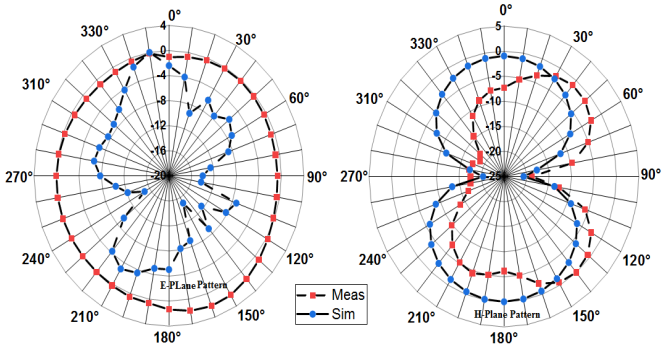

(i) (ii)

(d)

Fig.13. (a) 3D-Polar Pattern of SISO antenna at 3.6GHz (b) Gain polar plots of SISO antenna at 3.6GHz in (i)E-plane and (ii) H-planes with φ=0˚, φ=90 (c) 3D-Polar Pattern of 2X2MIMO antenna at 3.6GHz (d) Gain polar plots of MIMO antenna at 3.6GHz in (i) E-plane and (ii) H-planes with φ=0˚, φ=90˚

D. Resultant Parameters of MIMO Antenna

All resultant parameters of the 2-port MIMO antenna are represented in Table II with their measured values concerning their threshold values.

TABLE II
RESULTANT PARAMETERS OF CONCAVE-SHAPED 2X2MIMO ANTENNA

Parameter	Value	Threshold Value range
Reflection Coefficient, S11	-37.514dB at 3.54GHz	<-10dB (3.285-3.87GHz)
Fractional Bandwidth (FBW)	20.7% (3.285-3.87GHz)	<-10dB
Isolation Coefficient, S12	-30.3dB at 3.545GHz	<-15dB(3.0-4.0GHz)
Total Active Reflection Coefficient (TARC)	-31.402dB at 3.555GHz	<-10dB(3.3-3.83GHz) <-14dB(3.385-3.68GHz) <-20dB(3.46-3.62GHz) TARC<0: the antenna is suitable for diversity application
Impedance Bandwidth (BW)	14.87% <-10dB(3.3-3.83GHz) 8.35% <-14dB(3.385-3.68GHz) 4.52% <-20dB(3.46-3.62GHz)	<-10dB <-14dB <-20dB
VSWR_MIMO	<2(3.3->4GHz) <1.5(3.3-3.70GHz)	<2 <1.5
Envelope Correlation Coefficient(ECC)	0>ECC<0.0016 throughout the full range	<0.1(for better isolation) <0.3(pretty good) <0.1(should be for better isolation) =0.5 (ok) >0.5 (bad)
Cross-Correlation Coefficient(CCC)	$0<\sqrt{ECC}<0.000258$	----
Diversity Gain(DG)	9.994dB<DG<9.999dB	>9.95dB or close to 10dB
Radiation Efficiency ($\eta_{1,rad.}$) at port1 and ($\eta_{2,rad.}$) at port 2	67.12%< $\eta_{rad.}$<99.82%	$\geq$ 60% ($very\ good\ design$) and Close to 1(ideally)
Total Radiation Efficiency ($\eta_{rad.}$)	92.82%	------
Mean Effective Gain (MEG)	0.0173<MEG<0.0159	<±3dB
Radiation Efficiency ($\eta_{1rad.}$) at Port1	67.12%<($2XMEG_1$)<99.87%	-----
Radiation Efficiency ($\eta_{2rad.}$) at Port2	61.82%<($2XMEG_2$)<99.86%	-----
Group Delay, τ_g	<0.72ns	<0.5ns
Channel Capacity Loss (CCL)	0<CCL<0.4 Bits/sec/Hz (3.27-3.9GHz)	<0.4 Bits/sec/Hz
Gain (G)	3.38dBi	------
Directivity (D)	3.71dBi	------

E. RLC Equivalent Circuit of MIMO

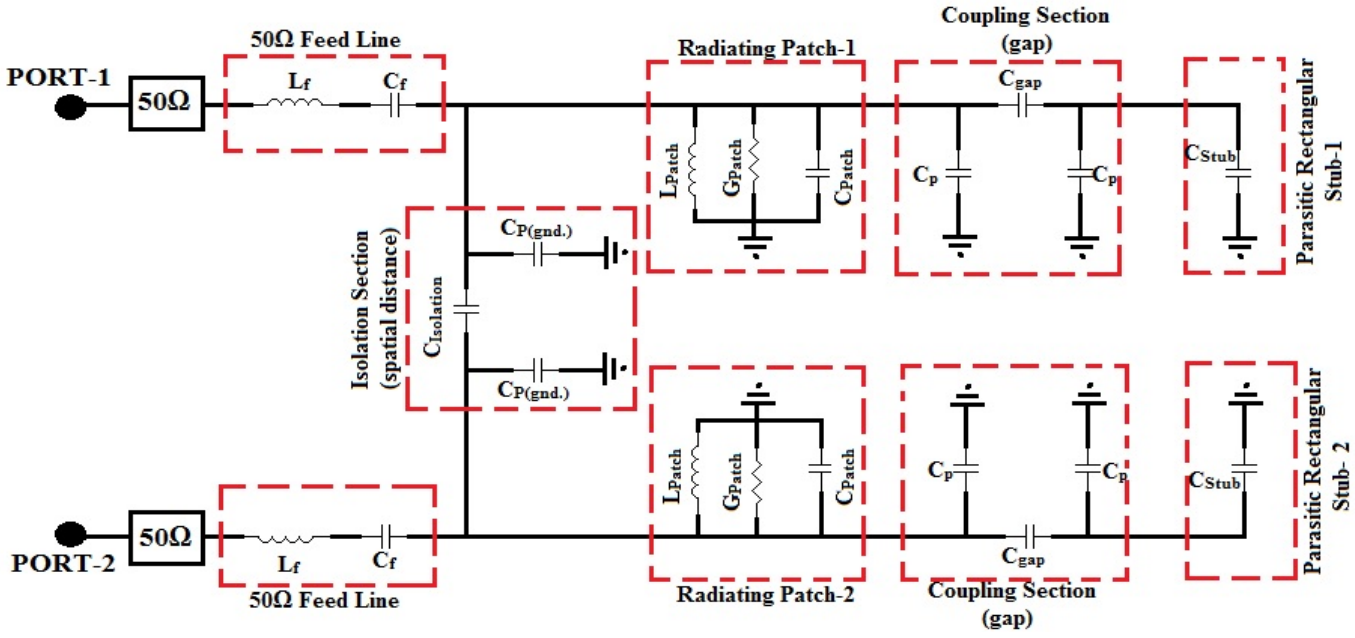

Fig.14. RLC Electrical Equivalent Circuit of the 2x2 MIMO antenna

The equivalent circuit is important to generate an analogy between lumped networks into distributed networks. The RLC electrical equivalent circuit of the proposed 2x2 MIMO antenna has been derived by considering the whole antenna structure into nine different sections. Since the two MIMO elements consist of two identical patches isolated by a spatial distance of 29.66mm apart; therefore only five sections are considered for calculations and rest four are having similar sections and hence similar RLC analysis because of identical patches. The proposed 2x2 MIMO comprises two 50Ω feed line sections, two concave-shaped radiating patches, two coupling gaps of 0.2mm, and two parasitic rectangular stubs with open ends. The estimation of the RLC parameters has been done by using formulas of references [16, 28]. The high isolation between the two antenna elements is represented by isolation caused due to the spatial distance arrangements. The two 50Ω feed line is represented by the series combinations of an inductance and a capacitance. The two patches are the parallel combination of patch conductance, patch inductance, and capacitance in the shunt arm. Further two air gaps exist between the rectangular stubs and patches, these cause more charges to accumulate periodically with opposite polarity and hence represented by a π-network with two shunt capacitances (due to ground). Open-end rectangular stubs show fringing at the open ends and are thus represented by fringing capacitance. All these capacitances are of value lower than 1pF. The Isolation between the two patches is also represented by isolation π-network having a gap capacitor because of the spatial distance between the two patches and two parallel shunt capacitances existing between radiating patches and the ground plane. The derived RLC electrical circuit is illustrated in Fig. 14 and their section-wise estimated RLC parameter values are displayed in Table IV.

TABLE III
RLC parameters of MIMO equivalent circuits

Section	Parameter Name	Value	Comment
Input Port (Two)	Port impedance	50Ω	For RF Input excitation
Feed line (Two No.)	R_f L_f C_f	0.00235Ω 1.30nH 0.666pF	Negligible R_f, i.e. short-circuited
Patch (Two No.)	G_{Patch} L_{Patch} C_{Patch}	$0.256X10^6$S 1.564nH 1.03pF	Negligible R_f, i.e. open circuited
Coupling (Gap=0.2mm) (Two No.)	C_{gap} $C_P=C_{P2}=C_{P1}$	7.46fF 12.18fF	Due to displacement current
Parasitic Rectangular Stubs (Two No.)	C_{Stub}	0.154pF	Due to the fringing length
Coupling (Gap=0.2mm) (Two No.)	$C_{Isolation}$ $C_P=C_{P2}=C_{P1}$	32.8fF 1.049pF	Due to spatial Distance

F. Performance Parameter Comparison of Existing Literature with Proposed Antenna

The performance parameter comparison of the proposed work with similar existing antennas (MIMO) is presented in Table IV. The MIMO antenna is compared with the other MIMO in terms of its normal parameters like gain, bandwidth, reflection coefficient, group delay, radiation efficiency, and other diversity performance parameters like Isolation, EEC, DG, CCL, MEG, etc.

IV. CONCLUSION

The proposed MIMO antenna has excellent isolation (<-30dB) and reflection coefficient values well below -10dB over the N-78 band (3.30-3.80GHz) wideband bandwidth, channel capacity loss (CCL<0.4bit/sec/Hz), envelope correlation coefficients (ECC<0.016), cross-correlation coefficient ($0<CCC=\sqrt{ECC}<0.000258$), diversity gain (9.994dB<DG<9.999dB), total active reflection coefficient (TARC= -31.402dB at 3.555GHz) corresponding VSWR-MIMO <2(3.3-4.2GHz) and <1.5(3.3-3.70GHz), mean effective gain (MEG<0.4dB) respectively, without the use of any additional electromagnetic band gap (EBG) structure, neutralize line, split ring resonators. The two radiating patches and DGS occupy very less area on the FR4 substrate. The minimum spatial distance between the two radiating patches is less than half wavelength. Thus, the 2x2 MIMO antenna is simple and very compact (miniaturized) in size. This may result in the possibility to connect extra passive components on the surface of the substrate. The radiation pattern of the antenna is Omnidirectional with a peak gain 3.38dBi and high radiation efficiency of 92.82%. The diversity performance parameter ECC is lower than 0.0016 and DG (>9.995dB) is close to 10dB, this ensures the reliability of the signal to reach the transmitter with a high data rate. A CCL lower than 0.4 bit/sec/Hz ensures an excellent signal-to-noise ratio (SNR) with the lowest interference at the far receiver end. In the future, because of the simplicity of the patch, the antenna can be used as 4x4 MIMO, 8x8 MIMO, or higher element massive MIMO systems.

V. RECOMMENDATION

It is noticed from the tabularized comparison that most literary works have been available without RLC-electrical equivalent circuits. The proposed 2x2 MIMO is presented an RLC electrical equivalent circuit with detailed descriptions of evaluated passive components. Therefore the proposed MIMO antenna is compatible with electrical networks easily. The antenna is fabricated on the low-cost FR-4 substrate, is simple in structure, and is developed from fractal technology, therefore this reduced ground monopole MIMO is easy to fabricate and replicate with 4x4 MIMO, 8x8 MIMO by adjustment of isolation. Alternatively, in the future, the stub-loaded MIMO antenna could be used with different orientations like vertically polarized and horizontally polarized to improve Isolation and TARC values. As

compared to available MIMO the proposed MIMO provides a platform to see all the MIMO parameters while others are available with fewer MIMO parameter considerations. The presented fractal 2x2 MIMO can be useful in wireless, military, and commercial applications as transitions, connectors, front-end RF elements, amplifiers, filters, transmitters, and receivers systems.

ACKNOWLEDGMENT

The authors are grateful to Hon'ble Vice-Chancellor, Gurukula Kangri (Deemed to be University), Haridwar, India for providing software and hardware support for the development of the MIMO project.

Availability of data and material The manuscript has no associated data.

Competing interests Authors declared that they have not received any form of funds or grants for the conduction of this research work.

Conflicts of interest Authors have no potential conflict of interest.

REFERENCES

[1] G. Saxena, P. Jain, and Y. K. Awasthi, "High Diversity Gain MIMO-Antenna for UWB Application with WLAN Notch Band Characteristic Including Human Interface Devices", *Wireless Personal Communications*, 2019, vol. 112, no. 1, pp. 105-121. DOI: 10.1007/s11277-019-07018-1

[2] D. El Hadri, A. Zakriti, A. Zugari, M. Ouahabi, and J. El Aoufi, "High Isolation and Ideal Correlation Using Spatial Diversity in a Compact MIMO Antenna for Fifth-Generation Applications", *International Journal of Antennas and Propagation*, 2020, vol. 1, pp. 1-10. DOI: 10.1155/2020/2740920.

[3] Q. Cai, Y. Li, X. Zhang, and W. Shen, "Wideband MIMO antenna array covering 3.3-7.1 GHz for 5G metal-rimmed smartphone applications", *IEEE Access,* 2019, vol. 7, pp. 142070-142084. DOI: 10.1109/ACCESS.2019.2944681

TABLE IV
PROPOSED MIMO PERFORMANCE COMPARISON WITH EXISTING MIMO ANTENNAS

[Refs] Type Antenna size (mm^3)	Substrate	S_{12} (dB)	-10-dB BW (GHZ)	Gain (dBi)	TARC (dB)	ECC	DG (dB)	CCL (bits/s/Hz)	Other	RLC Equivalent Circuit
[1] 2X2, 36X22X1.6	FR-4	<-30	3.1-11.2	7.0@ 5.6GHz	<-25	<0.004	>9.95	<0.3	MEG≈1dB τ_g:<0.3ns $\eta_{rad.}$:75-97%	Not given
[2] 2X2, 12.8X26X1.6	FR-4	<-35	27.5-28.3	6.68@ 28GHz	<-10	<0.0008	10	-----	$\eta_{rad.}$: 80%	Not given
[10] 2X2 and 4X4, 80X40X1.52	Taconic RF 30, tanδ= 0.0014, ε_r=3	<-20	3.18-11.5	-----	-----	<0.015	10	<0.4	-----	
[11] 2X2, 30X40X0.79	RT duroid 5880, ε_r=2.2, tanδ= 0.0009	<-20	2.8- 4.7 and 5.4 to more than 11	3.15-7.35	-----	<0.03 except 5-5.4GHz (notch band)	10 with a slight dip at 5.2 GHz	<0.25 Except few variations at 5.4 GHz	$\eta_{rad.}$: 85-96%	Not given
[12] 2X2, 45X80X1.2	FR-4	<-15	2.3-2.4	2.0 and 1.3	<-10	<0.16	-----	-----	MEG:<1.12 dB	Not given
[13] 2X2, 40X23X1.524	FR-4	<-25	2.5-10.4		<0	<0.0316	-----	<0.5	-----	
[14] 8X8, 20X8.7X0.4	FR-4	<-17	5.15-7.29	2.25	<-25	------	-----	-----	$\eta_{rad.}$>80% η_{total}> 70%	Not given
[26] 7X7, 64X32X0.508	Rogers RT5880	<-20	1.107 f_r=37.02	7.71	<-10	<0.01	9.95< DG<10	-----	Directivity:7.96 dBi MEG:3.01dB	Not given
[15] 2X2 64X38X1.27	Duroid, ε_r=2.2,	<-15	2.9-14.91	4.03	<-20	<0.0076	<10	-----	VSWR<2	Not given
[23] 2X2, 55X28X1.6	FR-4	<-29	2.01-3.92	3.55	<-10	<0.01	>9.8	<0.2	VSWR<2 MEG: ≈±0.3dB $\eta_{rad.}$>60%	Not given
[27] 2X2, 18X36X1.6	FR-4	<-18	3.0-40.0	0-4.0	<-10	<0.01	>9.98	-----	VSWR<2	Not given
Proposed 2X2, 53.66X24	FR-4	<-30	3.285-3.87	4.35@ 3.6GHz	-37.12	<0.016	>9.98	<0.4	MEG:<0.016 dB, τ_g:<0.72ns $\eta_{rad.}$: 92.82%	**Given**

[4] Z. Ren and A. Zhao, "Dual-band MIMO Antenna with Compact Self-Decoupled Antenna Pairs for 5G Mobile Applications", *IEEE Access*, 2019, vol. 7, pp. 82288-82296. DOI: 10.1109/ACCESS.2019.2923666

[5] M. Abdullah, Y.-L. Ban, -L., K. Kang, M.-Y Li, and M. Amin, "Eight-Element Antenna Array at 3.5 GHz for MIMO Wireless Application", *Progress in Electromagnetics Research C* (PIER-C), 2017, vol. 78, pp. 209-216. DOI: 10.2528/PIERC17082308

[6] H. Al-Saif, M. Usman, M. T. Chughtai and J. Nasir, "Compact Ultra-Wideband MIMO Antenna System for Lower 5G Bands", *Wireless Communications and Mobile Computing*, 2018, pp. 1-6. DOI:10.1155/2018/2396873

[7] T. S. Rappaport, Y. Xing, G. R. MacCartney, A. F. Molisch, E. Mellios and J. Zhang, "Overview of Millimeter Wave Communications for Fifth-Generation (5G) Wireless Networks with a Focus on Propagation Models", *IEEE Transactions on Antennas and Propagation*, 2017, vol. 65, no. 12, pp. 6213-6230. DOI: 10.1109/TAP.2017.2734243

[8] W. El-Halwagy, R. Mirzavand, J. Melzer, M. Hossain, and P. Mousavi, "Investigation of a Wideband Substrate-Integrated Vertically-Polarized Electric Dipole Antenna and Arrays for mm-wave 5G Mobile Devices", *IEEE Access*, 2017, vol. 6, pp. 2145-2157. DOI:10.1109/ACCESS.2017.2782083

[9] B. Fady, J. Terhzaz, A. Tribak, F. Riouch, and A. Sanchez Mediavilla, "Novel Miniaturized Planar Low-Cost Multiband Antenna for Industry 4.0 Communications", *Progress in Electromagnetics Research C, (PIER-C)*, 2019, vol. 93, pp. 29-38. DOI: 10.2528/PIERC19030809

[10] M. N. Hasan, S. Chu, S. Bashir, "A DGS monopole Antenna Loaded with U-shape Stub for UWB MIMO Applications", *Microw Opt Technol Lett.*, 2019, vol. 61, no. 9, pp. 2141-2149. DOI:10.1002/mop.31877

[11] D. Yadav, Mahesh, P. Abegaonkar, S. K. Koul, V. Tiwari and D. Bhatnagar, "Two Element Band-Notched UWB MIMO Antenna with High and Uniform Isolation", *Progress in Electromagnetics Research M (PIER M)*, 2018, vol. 63, pp. 119-129. DOI: 10.2528/PIERM17091106

[12] Y. Lee, D. Ga, and J. Choi, "Design of a MIMO Antenna with Improved Isolation Using MNG Metamaterial", *International Journal of Antennas and Propagation*, 2012, pp. 1-7. DOI: 10.1155/2012/864306.

[13] A. Quddus, R. Saleem, T. Shabbir, S. ur Rehman, and M. F. Shafique, "Dual Port UWB-MIMO Antenna with Ring Decoupling Structure", *Progress in Electromagnetic Research Symposium, (PIER S)*, Shanghai, China, 8–11 August 2016, vol. 37, pp. 116-119. DOI: 10.1109/PIERS.2016.7734262.

[14] J. Kulkarni and Chow-Yen-Desmond Sim, "Wideband CPW-Fed Oval-Shaped Monopole Antenna for Wi-Fi 5 and Wi-Fi 6 Applications", *Progress in Electromagnetics Research C,* (PIER-C), 2021, vol. 107, pp. 173-182. DOI: 10.2528/PIERC20110903

[15] E. A. Andrade-Gonzalez, J. C. Ordoñez-Martínez, M. Reyes-Ayala, J. A. M. Tirado, H. Terres-Peña, "Compact Fractal MIMO Antenna for UWB Applications", *WSEAS Transactions on Communications*, 2021, vol. 20, pp. 146-151. DOI: 10.37394/23204.2021.20.20

[16] C. A. Balanis, *Antenna Theory Analysis and Design*, 2nd ed., John Wiley and Sons, India, 2009.

[17] A. Varshney, N. Cholake, and V. Sharma, "Low-cost ELC-UWB Fan-Shaped Antenna Using Parasitic SRR Triplet for ISM Band and PCS Applications", *International Journal of Electronics Letters*, 2021 (online). DOI: 10.1080/21681724.2021.1966655

[18] T. K. Saha, C. Goodbody, T. Karacolak, and P. K. Sekhar, "A Compact Monopole Antenna for Ultra-Wideband Applications", *Microwave and Optical Technology Letter*, 2018, pp. 1-5. DOI: 10.1002/mop.31519

[19] M. Ahmed, Elshirkasi, Al-Hadi Azremi Abdullah, Mohd F. Mansor, Rizwan Kha and Ping J. Soh, "Envelope Correlation Coefficient of a Two-Port MIMO Terminal Antenna under Uniform and Gaussian Angular Power Spectrum with User's Hand Effect", *Progress in Electromagnetics Research C, 92 (PIER C)*, 2019, pp. 123-136. DOI: 10.2528/PIERC19011006

[20] X. Wang, H. D. Nguyen, and H. T. Hui, "Correlation Coefficient Expression by S-parameters for Two Omnidirectional MIMO Antennas", *IEEE International Symposium on Antennas and Propagation (APSURSI)*, 2011, pp. 301-304. DOI:10.1109/APS.2011.5996702

[21] Y. K. Choukiker, S. K. Sharma, S. K. Behera, "Hybrid Fractal Shape Planar Monopole Antenna Covering Multiband Wireless Communications with MIMO Implementation for Handheld Mobile Devices", *IEEE Transactions on Antennas and Propagation*, 2014, vol. 62, no. 3, pp. 1483-1488. DOI: 10.1109/TAP.2013.2295213

[22] H. S. Singh, "Investigations of MIMO Antenna for Smart Mobile Handsets and Their User Proximity", *Intech Open*, 2019, pp. 23-32. DOI:10.5772/intechopen.75002.

[23] A. K. Biswas, U. Chakraborty, "Reduced Mutual Coupling of Compact MIMO Antenna Designed for WLAN and WiMAX Applications", *International Journal of RF and Microwave Computer-Aided Engineering*, 2019, vol. 29, no. 3, pp. 1-10. DOI: 10.1002/mmce.21629

[24] Tathababu Addepalli, Arpan Desai, Issa Elfergani, N. Anveshkumar, Jayshri Kulkarni, Chemseddine Zebiri, Jonathan Rodriguez and Raed Abd-Alhameed, "8-Port Semi-Circular Arc MIMO Antenna with an Inverted L-Strip Loaded Connected Ground for UWB Applications", *Electronics*, 2021, vol. 10, no. 12, pp. 1-19. DOI: 10.3390/electronics10121476.

[25] J.-Y. Chung, T. Yang, and J. Y. Lee, "Low Correlation MIMO Antennas with Negative Group Delay", *Progress In Electromagnetics Research-C*, 2011, vol. 22, pp. 151-163. DOI: 10.2528/PIERC11051007

[26] M. J. Riaz, et al., "MIMO Antennas for Future 5G Communications", *IEEE 23rd International Multitopic Conference (INMIC)*, Bahawalpur, Pakistan, 2020. DOI: 10.1109/INMIC50486.2020.9318126

[27] M. I. Khan, M. I. Khattak, S. U. Rahman, A. Qazi, B. A. Telba, A. Sebak, "Design and Investigation of Modern UWB-MIMO Antenna with Optimized Isolation", *Micromachines*, 2020, vol. 11, no. 4, pp. 1-11. DOI: 10.3390/mi11040432.

[28] T.C. Edward and M. B. Steer, *Foundation for Microstrip Circuit Design*, 4th ed., Wiley IEEE Press, 2016.

[29] P. V. Naidu, D. Maheshbabu, A. Saiharanadh, A. Kumar, N. Vummadisetty, L. Sumanji, and K. A. Meerja, "A Compact Four-Port High Isolation Hook Shaped ACS Fed MIMO Antenna for Dual Frequency Band Applications," *Progress In Electromagnetics Research C*, 2021, vol. 113, pp. 69-82. DOI: 10.2528/PIERC21042701